

**High-temperature desorption of  $C_{60}$  covalently bound to  $6H$ -SiC(0001)- $(3 \times 3)$** 

F. C. Bocquet, Y. Ksari, L. Giovanelli, L. Porte, and J.-M. Themlin\*

*Aix-Marseille Univ, IM2NP, 13397, Marseille, France**CNRS, IM2NP (UMR 6242), 13397, Marseille-Toulon, France*

(Received 17 January 2011; revised manuscript received 18 July 2011; published 16 August 2011)

The desorption or fragmentation temperature of  $C_{60}$  bound to Si-rich- $(3 \times 3)$  and  $(\sqrt{3} \times \sqrt{3})R30^\circ$  reconstructions of  $6H$ -SiC(0001) is investigated using inverse photoemission spectroscopy (IPES) and LEED experiments. On SiC- $(3 \times 3)$ ,  $C_{60}$  film is found desorbed after annealing at a high temperature of 1140 K, supporting covalent bonding. Meanwhile, the Si tetramers of the  $(3 \times 3)$  nanostructured substrate are recovered, as can be inferred from the full reappearance of the Mott-Hubbard surface state in the IPE spectra. SiC- $(3 \times 3)$  behaves in a singular way among the other semiconducting substrates, which covalently bind to  $C_{60}$ . This remarkable feature is attributed to the low density of Si dangling bonds and to the highly corrugated character of this reconstruction.

DOI: [10.1103/PhysRevB.84.075333](https://doi.org/10.1103/PhysRevB.84.075333)

PACS number(s): 68.43.Vx, 68.55.ap, 73.20.-r, 68.35.bg

**I. INTRODUCTION**

Silicon carbide (SiC) is a wide band gap semiconductor with many promising qualities for future applications.<sup>1</sup> Its high breakdown electric field and thermal conductivity renders it a good candidate for fast and high-power electronic devices. The scientific interest for SiC has increased in recent years and intensified since it was discovered that one or several epitaxial graphene overlayers form when SiC is annealed above 1500 K (for a recent review see Ref. 2). It is also well known that SiC forms by thermal decomposition of  $C_{60}$  adsorbed on either Si(111)- $(7 \times 7)$  (see Refs. 3 and 4) or Si(100)- $(2 \times 1)$  reconstructed surfaces.<sup>4,5</sup> Therefore, it can be expected that a two-step process may allow high-quality graphene fabrication using  $C_{60}$  and Si substrates, which are both of low cost.

The rich field of fullerene adsorption on semiconductor surfaces is currently very active.<sup>6,7</sup> Regarding  $C_{60}$  adsorption on Si surfaces, on both Si(111)- $(7 \times 7)$  and Si(100)- $(2 \times 1)$ , scanning tunneling microscopy (STM) experiments showed that there is no extended  $C_{60}$  superstructures formation. This fact is attributed to the strong, predominantly covalent, interaction<sup>8</sup> between the molecules and the substrates, which limits the surface diffusion. In some experiments, a charge transfer<sup>9,10</sup> from the substrate to the molecules was also inferred.

Only a few studies were devoted to  $C_{60}$  adsorption on SiC surfaces.<sup>6</sup> We will consider the sole STM study of  $C_{60}$  adsorption on the Si-rich  $(3 \times 3)$  and  $(\sqrt{3} \times \sqrt{3})R30^\circ$  reconstructions.<sup>11</sup> Among several equilibrium structures of the polar (Si-terminated) (0001) faces of the hexagonal SiC polytypes, these surfaces are two Si-rich reconstructions,<sup>12</sup> which are structurally very different. The  $(3 \times 3)$  reconstruction has been predicted by DFT-local-density-approximation (DFT-LDA) calculations to be the minimum free-energy structure under Si-rich preparation conditions.<sup>13</sup> It involves a twisted Si-adlayer above a Si-terminated SiC substrate, with Si tetramer adclusters on top separated by 9.24 Å. This reconstruction is characterized by a large Si coverage of 13/9 (see Ref. 12). By contrast, the less Si-rich  $(\sqrt{3} \times \sqrt{3})R30^\circ$  reconstruction can only be stabilized for not too Si-rich preparation conditions, and is typically obtained upon annealing a  $(3 \times 3)$  reconstruction. It has a simpler structure involving

Si-adatoms localized in  $T_4$  sites, separated by 5.3 Å, on top of the outermost C-Si bilayer.<sup>14</sup> Both terminations exhibit one half-filled dangling orbital per surface unit cell, more commonly called a “dangling bond” (DB), mostly localized on the Si adatom [the Si atom at the apex of the tetramers for the  $(3 \times 3)$  reconstruction]. As a common peculiarity due to the large separation between dangling bonds, the associated surface states show large correlation effects and both systems share a Mott-Hubbard insulator ground state, although with a different U parameter.<sup>15,16</sup>

In the present work, we consider the adsorption, anchoring and decomposition/desorption mechanisms of  $C_{60}$  on these Si-rich  $(3 \times 3)$  and  $(\sqrt{3} \times \sqrt{3})R30^\circ$  reconstructions of  $6H$ -SiC(0001) upon annealing. Being structurally very different, these two surfaces are expected to manifest different reactivities toward  $C_{60}$  adsorption and a different behavior when the molecules adopt more stable adsorption configurations upon annealing at increasing temperatures. The bonding strength of  $C_{60}$  adsorbed at room temperature on both reconstructions has been studied by annealing a  $C_{60}$  thick film (TF) at increasing temperatures until  $C_{60}$  desorption or fragmentation happens. Low-energy electron diffraction (LEED) and inverse photoemission spectroscopy (IPES) experiments were performed. IPES probes the unoccupied electronic structure near the Fermi level ( $E_F$ ). It is a convenient technique for the purpose of this investigation mainly because the large and highly symmetrical  $C_{60}$  molecule leads to sharp IPE peaks in this energy domain.<sup>17</sup> As a surface-sensitive technique, it allows to discriminate a truly clean surface from a surface contaminated with reacted molecular fragments. One full  $C_{60}$  monolayer is able to quench the IPE signal from the covered substrate to a hardly detectable value. This assumption was also made in some previous experimental IPE studies when  $C_{60}$  deposition was involved.<sup>21,37</sup>

**II. EXPERIMENTS AND SURFACE PREPARATION**

The experiments were performed in ultrahigh vacuum (UHV) conditions (base pressure of  $\sim 2 \times 10^{-10}$  mBar) and all the measurements were done at room temperature. IPES experiments were performed using a homemade spectrometer

described in Ref. 18. The spectra present the photon yield (at  $h\nu = 9.7$  eV) normalized to the sample current with typical current values in the  $\mu\text{A}$  range. The Fermi level  $E_F$  was calibrated using a clean Ta sample. The temperature was calibrated using an infrared pyrometer with  $\pm 25$  K uncertainty. A rectangular  $n$ -doped SiC sample from Sterling Semiconductors with  $N_D = 9 \times 10^{17} \text{ cm}^{-3}$  has been used. Several  $(3 \times 3) \rightarrow (\sqrt{3} \times \sqrt{3})R30^\circ \rightarrow (3 \times 3)$  cycles were performed in order to desorb oxidized species and also to find the optimized conditions of preparation for each studied surface. The SiC- $(3 \times 3)$  is obtained by annealing the SiC substrate at  $\sim 1120$  K under a Si flux generated by a Si wafer placed nearby the sample and resistively heated at  $\sim 1420$  K. During a second step, the substrate is annealed at the same temperature without any Si flux in order to evacuate excess Si atoms and also improve the surface crystal structure. The substrate temperature, Si flux, and annealing times were adjusted until sharp LEED patterns with low background could be obtained. Starting from a  $(3 \times 3)$  surface, the  $(\sqrt{3} \times \sqrt{3})R30^\circ$  reconstruction was obtained by annealing the SiC substrate for a few minutes at  $\sim 1170$  K without any Si flux. Each reconstruction has characteristic IPE features and can therefore be well identified.<sup>19</sup>

$\text{C}_{60}$  deposition was performed using a carefully degassed Knudsen cell. During molecule evaporation the temperature cell was maintained at 668 K. The film thickness was roughly calibrated using an Inficon quartz microbalance. The evaporation temperature mentioned above corresponds to a deposition rate of  $\sim 0.05$  ML/min, which is in the range used by other authors for the study of  $\text{C}_{60}$  interaction with some other surfaces<sup>20,21</sup> using photoemission experiments (ML stands for monolayer). The molecular depositions were performed with the  $6H$ -SiC(0001) substrate held at room temperature. To avoid the difficulties due to the definition of 1 ML (see Ref. 11) the following experimental protocol was followed. A thick  $\text{C}_{60}$  film was deposited over a clean surface. Different successive annealings were then performed for a duration of 10 min at increasing temperatures up to 1200 K. According to Goldoni *et al.*,<sup>22</sup> a characteristic time of 800 s is needed for the chemical reaction of  $\text{C}_{60}$  on Si(111)- $(7 \times 7)$  at 1035 K. The 10-min annealing time used here is then long enough to observe any film modification (fragmentation or desorption). It is however short enough<sup>23</sup> to prevent the evolution of the underlying  $(3 \times 3)$  surface here prepared at 1120 K. Since the  $(\sqrt{3} \times \sqrt{3})R30^\circ$  is obtained using a few-min annealing at 1170 K, one can expect that a longer annealing time at a temperature between 1120 and 1170 K without Si supply can already alter the  $(3 \times 3)$  reconstruction.

### III. RESULTS

#### A. $\text{C}_{60}/6H\text{-SiC}(0001)\text{-}(3 \times 3)$

The crystallographic structure of SiC- $(3 \times 3)$  consists of Si-tetramers arranged in a hexagonal array with 9.24-Å lattice parameter covering a Si adlayer on top of a Si termination.<sup>13,25</sup> The  $(3 \times 3)$  reconstruction of SiC is therefore a surface solely made of Si. As the  $\text{C}_{60}$  coverage increases, the LEED spots due to the underlying  $(3 \times 3)$  reconstruction progressively weaken and disappear, a diffuse background being the only

visible trace on the LEED screen. It was not possible to identify extra-LEED spots, which would reveal an ordered  $\text{C}_{60}$  superstructure. In order to evaluate the bonding strength, a TF layer was deposited and annealed at increasing temperatures between room temperature and 1140 K. The IPES spectra are shown in Fig. 1(a). From the bottom to the top, the clean surface spectrum, the as-deposited TF spectrum, and the spectra corresponding to the different annealing steps at increasing temperatures are displayed. The clean surface spectrum can be fitted using six components in the energy range 0–8.1 eV as revealed by previous studies.<sup>19,24</sup> The  $(3 \times 3)$  surface should be metallic according to one-electron band-theory but experiments show that it is an insulator.<sup>26</sup> Thus the low-lying IPE peak located at  $(0.6 \pm 0.1)$  eV (peak-a) was attributed to the upper band of a Mott-Hubbard electron state<sup>27</sup> localized at the apex of the Si tetramers. To our knowledge, the origin of the other five peaks (b to f) has still not been determined: ascribing one of these IPE peaks to a particular surface or bulk density of states remains an open issue. Some differences in the overall shape of various normal incidence IPE spectra of the  $(3 \times 3)$  reconstruction may be evidenced by a careful examination of published IPES spectra.<sup>19,24,27</sup> Slightly different preparation conditions (annealing time, annealing temperature, cooling profile, Si flux, etc.) may also influence the homogeneity of the  $(3 \times 3)$ -terraces, thus affecting the overall shape of IPE spectra. Provided this variability, we thoroughly checked the reproducibility of the presented results and showed in Fig. 1(a) a set of representative spectra.

In order to address the interface bonding, we briefly recall some inverse photoemission results for solid  $\text{C}_{60}$ . The origin of the first three low-lying features labeled 1–3 in Fig. 1 was discussed in Refs. 17 and 28. Feature 1 band center appears at  $(1.5 \pm 0.1)$  eV above  $E_F$ , in good agreement with previous results.<sup>17,29</sup> The states contributing to peak 2 have more wave-function overlap than those contributing to the adjacent peaks.<sup>17</sup> This IPE peak is thus expected to be particularly sensitive to the interaction of  $\text{C}_{60}$  with the substrate or between neighboring molecules. Well-developed peak 2 together with long evaporation duration ( $\geq 1$  hour) and quartz monitoring were used as complementary criterions to ascertain that a thick enough  $\text{C}_{60}$  layer was effectively deposited.

After annealing at  $\sim 650$  K, the outermost  $\text{C}_{60}$  layers readily desorbed exposing the interface layer in close contact with the substrate. The main modifications on the TF  $\text{C}_{60}$  electronic structure are a strong reduction of the peak 2 intensity accompanied by a decrease of peak 1 to peak 3 splitting (upward shift of peak 1, downward shift of peak 3), and an overall broadening with respect to the TF. This effect is attributed later on to covalent bonding of the fullerene in contact with the substrate.

Further annealing at 860 K did not substantially modify the IPES spectrum. For the sake of clarity, only the spectrum at 860 K is shown in Fig. 1(a). After annealing at  $\sim 1040$  K, a  $(1 \times 1)$  LEED pattern with faint spots and large diffuse background appears (not shown). In the meantime, molecular features weaken gradually and some IPE intensity appears in the energy domain resonant with the energies of the peaks e and f of the clean substrate. This tendency is confirmed

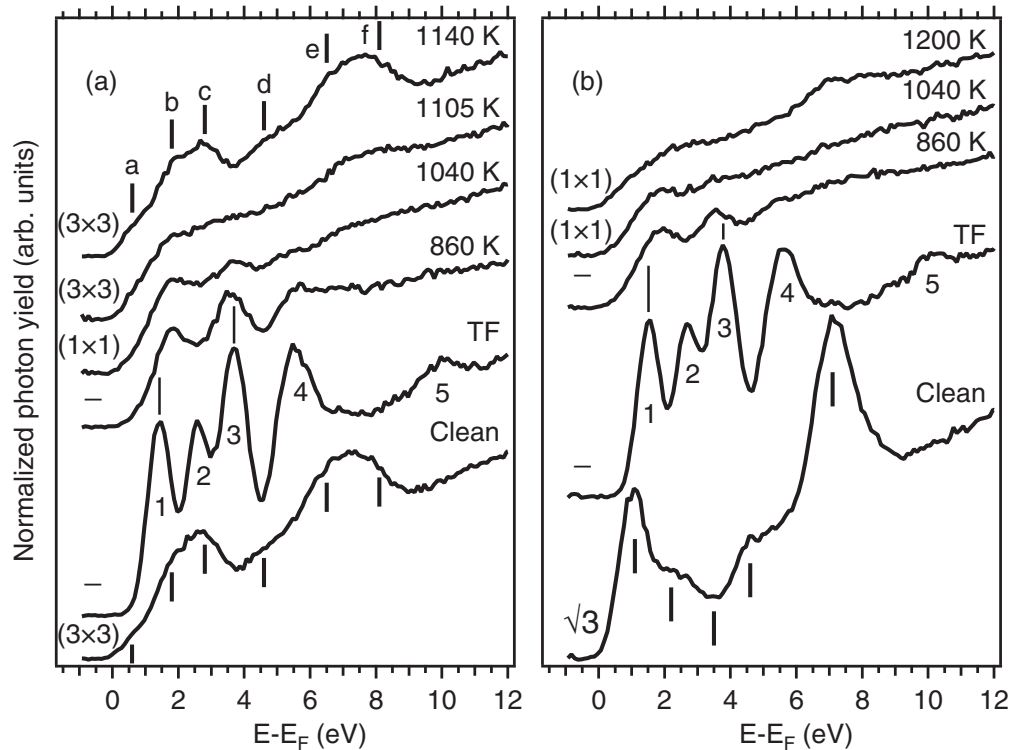


FIG. 1. Evolution of the normal incidence IPE spectra after annealing the  $(3 \times 3)$  and  $(\sqrt{3} \times \sqrt{3})R30^\circ$  reconstruction covered with a  $C_{60}$  TF in (a) and (b), respectively. From the bottom to the top: clean reconstruction spectra and  $C_{60}$  TF and annealed films. Vertical thick bars show the energies of the IPE peaks of the clean reconstruction, as reported in Ref. 24, with the same labels a–f. Vertical thin bars allow comparison of peak 1 (peak 3) energies before and after annealing  $C_{60}$  film. For each spectrum, the corresponding annealing temperature and LEED pattern are indicated on the right and left part of each panel, respectively. In (b) the spectrum corresponding to the clean surface is labeled  $\sqrt{3}$ .

after the annealing at  $\sim 1100$  K: the molecular features have almost disappeared while the high-energy contribution from the substrate is now emerging. In parallel, a  $(3 \times 3)$  LEED pattern becomes visible revealing the presence of large uncovered regions of a reconstructed substrate. After the last annealing at  $\sim 1140$  K, a  $(3 \times 3)$  LEED pattern presented in Fig. 2 with spots as sharp as the ones of the clean  $(3 \times 3)$  substrate is recovered, with similar diffuse background levels. Furthermore, the corresponding IPE spectra also appear very similar. All six peaks characteristic of a clean  $(3 \times 3)$  substrate are present in the spectrum of the high-temperature annealing, including the low-lying one (at  $\sim 0.6$  eV). The fact that this surface state appears fully recovered shows that no molecular fragments remain bound to the Si adclusters. As discussed later, the majority of molecules appear to desorb without significant dissociation despite the fact that a rather high temperature above 1100 K is needed. Before deposition, the clean  $(3 \times 3)$  surface contains inevitably a small proportion of defects. After the deposition and the annealing at 1140 K, these defects may induce the dissociation of a small proportion (not quantifiable here) of molecules. Nonetheless, our spectroscopic results support a large-scale thermally activated desorption process above 100 K. This temperature is actually higher than the dissociation temperatures of 1050, 1020, and 870 K at which covalently bound  $C_{60}$  decomposes on  $\text{Si}(110)$ - $(7 \times 7)$ ,<sup>22</sup>  $\text{Si}(100)$ - $(2 \times 1)$ ,<sup>5</sup> and  $\text{Si}(110)$ - $(16 \times 2)$ ,<sup>30</sup> respectively. As explained later, this intriguing fact may be related to the peculiarities of the  $(3 \times 3)$  reconstruction, in

particular the low density of its reactive sites. Finally, the  $(3 \times 3)$  reconstruction recovered after desorption, like the pristine one, naturally evolves toward a  $(\sqrt{3} \times \sqrt{3})R30^\circ$  when the substrate is further annealed using the conditions described in the previous section.

### B. $C_{60}/6H\text{-SiC}(0001)$ - $(\sqrt{3} \times \sqrt{3})R30^\circ$

Figure 1(b) shows the IPES results for the  $(\sqrt{3} \times \sqrt{3})R30^\circ$  surface. The bottom spectrum labeled  $\sqrt{3}$  corresponds to the freshly-prepared surface. The low-energy peak at  $(1.1 \pm 0.1)$  eV above  $E_F$  was attributed to a Mott-Hubbard state localized on Si adatoms,<sup>31–33</sup> forming a triangular lattice of DBs with a lattice parameter of 5.3 Å. Its sharpness is indicative of the good quality of the surface reconstruction.<sup>31</sup> To our knowledge, the origin of the four IPE peaks<sup>24</sup> standing in energy above the low-lying one has still not been determined. Since exposition to residual atmosphere of the UHV chamber modifies the IPE spectrum quite rapidly,<sup>24</sup> a TF layer was deposited as soon as the LEED and IPE acquisition for a clean surface were finished. Successive annealings were then performed. As for the  $(3 \times 3)$  surface, there is no detectable LEED spots due either to the substrate or to the remaining interface layer, after the outermost  $C_{60}$  were desorbed. After the annealing at  $\sim 860$  K, it can be seen that the  $C_{60}$  electronic structure with respect to the TF is perturbed in the same way as for the  $(3 \times 3)$  surface (i.e., strong peak 2 intensity reduction with a decrease of peak 1



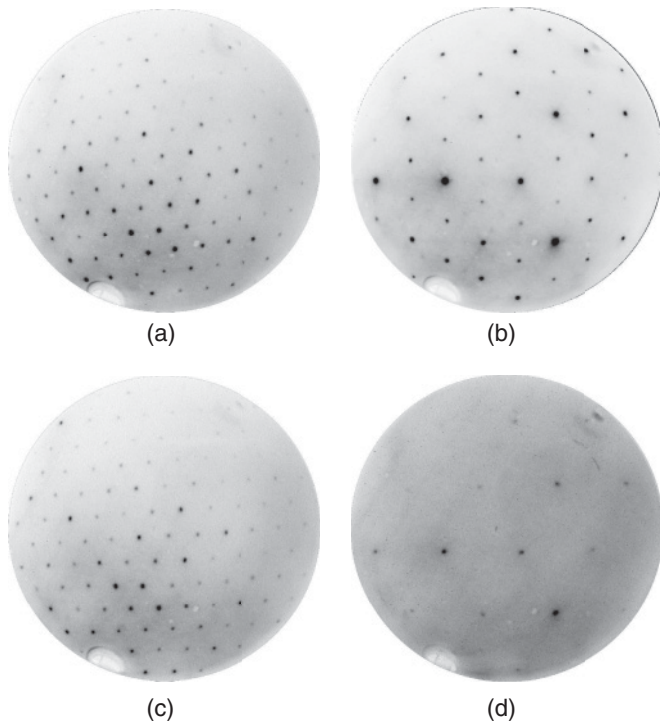


FIG. 2. LEED patterns for the SiC- $(3 \times 3)$  ( $E_p = 140$  eV) and SiC- $(\sqrt{3} \times \sqrt{3})R30^\circ$  ( $E_p = 180$  eV) reconstructions before  $C_{60}$  deposition and after annealing a  $C_{60}$  TF. Top left: clean  $(3 \times 3)$ , bottom left: after annealing a TF over  $(3 \times 3)$  at 1140 K. Top right: clean  $(\sqrt{3} \times \sqrt{3})R30^\circ$ , bottom right after annealing a TF over  $(\sqrt{3} \times \sqrt{3})R30^\circ$  at 1200 K, note the strong diffuse background.

to peak 3 splitting both peaks shifting toward each other and overall peak broadening<sup>4</sup>). After the annealing at  $\sim 1040$  K, a few  $(1 \times 1)$  LEED spots with weaker intensity and a rather large diffuse background appeared (not shown). Two weak features are still visible in the IPE spectrum corresponding to peak 1 and peak 3. At last, after further annealing up to  $\sim 1200$  K, there is no feature attributable to  $C_{60}$  in IPE and no improvement of the LEED pattern can be seen with comparison to the LEED pattern obtained after the  $\sim 1040$ -K annealing. The shape of the IPE spectrum is then very similar to the shape of a  $(1 \times 1)$  surface<sup>19</sup> IPE spectrum. These results indicate that at high temperature, the  $C_{60}$  molecules fragment over the  $(\sqrt{3} \times \sqrt{3})R30^\circ$  reconstruction, possibly reacting with the Si adatoms in  $T_4$  sites and forming SiC as happens with the Si(111)- $(7 \times 7)$  and Si(100)- $(2 \times 1)$  surfaces. Finally, for both substrates studied here and for various incidence angles (not shown), there is no measurable density of states at the Fermi level for the annealed  $C_{60}$  layer that keeps an insulating behavior.

#### IV. DISCUSSION

The adsorption of  $C_{60}$  on single-crystal surfaces was the subject of a number of studies. Maxwell *et al.* have summarized the results in a comprehensive paper<sup>8</sup> in which a schematic picture of the different kind of molecule-substrate interactions was proposed. Although no clear boundary can be settled between different kind of adsorption mechanisms, the cited paper can be used as a useful framework. The

desorption (or fragmentation) temperature is used as a measure of substrate-adsorbate bonding strength. Accordingly, the surfaces are classified into three main categories: weak (I), intermediate (II), or strong (III) for a predominantly van der Waals, ionic, or covalent bonding, respectively. Although a few exceptions were mentioned, basically the different surfaces can be assigned to one of these three categories. For semiconductor surfaces, two categories are mentioned. When no dangling bonds are present, the interaction is of van der Waals type and the desorption temperatures are low (category I). For Si- and Ge- reconstructed surfaces, see Refs. 8 and 20, respectively, the molecules do not desorb intact but rather dissociate at high temperature (category III). In the following, we will try to rationalize the results of the present study within the depicted frame.

The desorption temperature for the category II substrates is in the range 700–800 K<sup>8</sup> if we discard Ag(100) for which a strong predominantly ionic bonding was inferred.<sup>34</sup> SiC- $(3 \times 3)$  and  $(\sqrt{3} \times \sqrt{3})R30^\circ$  do not belong to category II, first, because we do not observe any desorption of the first layer in this range. Moreover, for category II,  $C_{60}$  is found to be mobile<sup>8</sup> on the surface at room temperature and this was proven not to be the case by Li *et al.*<sup>11</sup> who found no sign of  $C_{60}$  diffusion at low coverage on both surfaces. Finally,  $C_{60}$  submolecular structures were resolved on their STM images of the  $(\sqrt{3} \times \sqrt{3})R30^\circ$ .<sup>11</sup> Their results indicate that there is little or no mobility at room temperature.

In the following, we therefore focus on category III, which is used to describe strong and predominantly covalent bonding. For these surfaces, the  $C_{60}$  dissociation happens at much higher temperatures, in the range 1000–1100 K.<sup>8</sup> For all the surfaces of category III, the strong bonding drives the molecular dissociation at high temperature with formation of a carbidic layer. For Ge(111), Bertoni *et al.*<sup>20</sup> showed that above 970 K,  $C_{60}$  dissociates and desorbs with restoration of a rather diffuse substrate LEED pattern. In the same time, a significant amount of carbon atoms still remains on the substrate ( $\sim 0.1$  ML). To our knowledge, there are, therefore, no examples inside category III of covalent bonding with  $C_{60}$  desorption and full recovery of the underlying reconstruction.

We come now to the surfaces of the present study. The  $6H$ -SiC(0001)- $(\sqrt{3} \times \sqrt{3})R30^\circ$  reconstruction should obviously be considered as new member inside category III. The spectroscopic results shown here present many similarities with those of Refs. 35 and 4 for  $C_{60}$  adsorbed on Si(111)- $(7 \times 7)$ : after a mild annealing, a reduction of peak-2 intensity and a decrease of peak-1 to peak-3 splitting is evidenced. A broadening of the molecular spectral components is also found. Since it is widely considered that the bonding with the Si(111)- $(7 \times 7)$  surface has covalent character<sup>8,22,35,36</sup> (at least after annealing), we assume that such picture also holds for the SiC  $(\sqrt{3} \times \sqrt{3})R30^\circ$  reconstruction. There is, at the present time, no consensus about the physisorbed or chemisorbed nature of the bonding between as-deposited  $C_{60}$  at  $\sim 1$  ML and Si(111)- $(7 \times 7)$ .<sup>6</sup>

At intermediate temperatures, the electronic structure of  $(3 \times 3)$  and  $(\sqrt{3} \times \sqrt{3})R30^\circ$  are basically perturbed in the same way, indicating that the bonding of  $C_{60}$  to  $(3 \times 3)$  is also predominantly covalent. However, from that point, a specific scenario should be invoked for the  $(3 \times 3)$  surface, since upon

annealing at 1140 K, our experimental results support a full desorption of the adsorbate. Moreover, we infer from the IPE spectra that the  $(3 \times 3)$  structure is either preserved or recovered because the unoccupied surface electronic structure appears very similar to the pristine reconstruction. It is at the present stage clear that the  $(3 \times 3)$  reconstruction is singular when compared to  $(\sqrt{3} \times \sqrt{3})R30^\circ$  of  $6H$ -SiC(0001) and also to both Si(111) and (100) surfaces. To our knowledge, as far as C<sub>60</sub> adsorption is concerned, the  $(3 \times 3)$  is a singular example of strong predominantly covalent bonding with the possibility of recovering the original reconstruction after desorption.

It is naturally tempting to attribute the special behavior of the  $(3 \times 3)$  reconstruction to the very small density of Si DB covering the surface. In Table I, we compare the DB density of four Si-terminated SiC and Si surfaces. It can be seen that it is precisely for the SiC- $(3 \times 3)$  reconstruction that the DB density is the smallest (with an area of 75 Å<sup>2</sup> per DB). For SiC- $(\sqrt{3} \times \sqrt{3})R30^\circ$ , this parameter lies in between the values of Si(100) and Si(111), all three values being much smaller than the 75 Å<sup>2</sup> per DB on  $(3 \times 3)$ . Pioneering fast photoemission studies by Goldoni *et al.*<sup>22</sup> on Si surfaces have already shown the importance of thermally induced deformed molecular species, which are precursors of C<sub>60</sub> dissociation and subsequent SiC formation. Indeed, when Si(111) surfaces are annealed at high temperatures, flattened fullerenes are stabilized by additional C<sub>60</sub> substrate bonds, as numerous as 20 bonds per C<sub>60</sub> before molecular dissociation can occur.<sup>4,5,22</sup> The formation of Si<sub>x</sub>C<sub>60</sub> results in weakened intramolecular C-C bonds, which eases the subsequent steps of molecular decomposition and SiC formation. The anchoring of the deformed precursor appears naturally favored by a high density of reactive DB at the surface. Considering the number of additional bonds with regards to the molecular size, it has also been suggested that some surface Si atom bonds break to allow the formation of extra Si-C bonds. In this respect, the highly corrugated character of the cluster-based  $(3 \times 3)$  reconstruction obviously limits the number of available Si atoms at the vicinity of the initial adsorption site. We hypothesize that if the deformed precursors are not sufficiently anchored to the substrate, they are able to leave it before molecular decomposition may occur. Our result do show that a  $(3 \times 3)$  reconstruction is recovered by annealing up to 1140 K, including the Si-adatoms which are responsible for the Mott-Hubbard surface state. Recent XPS and STM experiments support our interpretation. We surmise that the Buckyballs may desorb molecularly, although we did not directly analyze the desorption products.

TABLE I. DB specific area and surface composition of different Si and SiC(0001) surfaces after high-temperature annealing of deposited C<sub>60</sub> film.

Surface	DB specific area (Å <sup>2</sup> /DB)	Above 1140 K
$6H$ -SiC(0001)- $(3 \times 3)$	~75	Pristine $(3 \times 3)$
$6H$ -SiC(0001)- $(\sqrt{3} \times \sqrt{3})R30^\circ$	~25	SiC formation
Si(111)-(7 × 7)	~33	SiC formation
Si(100)-(2 × 1)	~15	SiC formation

Part of our results may seem conflicting with the interpretation of the STM results reported by Li *et al.*<sup>11</sup> These authors suggest that a single C<sub>60</sub> layer adsorbed on the  $(3 \times 3)$  decomposes upon annealing at 1120 K forming SiC islands. Annealing 1 ML C<sub>60</sub> adsorbed on the  $(3 \times 3)$  at 850 °C (1123 K) is reported<sup>11</sup> to lead to the growth of SiC islands following C<sub>60</sub> decomposition. The observation of irregularly shaped clusters upon annealing above 600 °C at 0.02 ML is said to support the C<sub>60</sub> decomposition and/or C<sub>60</sub>-Si clusters formation. However, a further annealing at 1000 °C (1273 K) is reported to induce the growth of larger SiC clusters with a  $(\sqrt{3} \times \sqrt{3})R30^\circ$  reconstruction (without external Si supply). Our results unambiguously show that, between these two temperatures (1123 and 1273 K) where STM images were reported, a  $(3 \times 3)$  reconstruction can be fully recovered after desorption. This  $(3 \times 3)$  reconstruction naturally evolves toward a  $(\sqrt{3} \times \sqrt{3})R30^\circ$  upon annealing at temperatures close to 1270 K, as is the case for an uncovered substrate. This is a further indication of the full desorption of any adsorbed species. In accordance to our results, annealing a multilayer of C<sub>60</sub> adsorbed on the  $(\sqrt{3} \times \sqrt{3})R30^\circ$  did not induce the formation of any ordered structure, and the C<sub>60</sub> or SiC clusters could not be desorbed by annealing at temperatures as high as 1323 K.

In the light of the present results, we propose to divide the surfaces of category III sharing the common property of strong, predominantly covalent, bonding into two subcategories. A category IIIA inside of which we find surfaces driving C<sub>60</sub> dissociation at high temperature and a category IIIB containing surfaces remaining reconstructed and quasifree of residual carbon fragments after desorption. In the case of Ge(111) already mentioned above, there is some evidence from photoemission measurements for C<sub>60</sub> dissociation.<sup>20</sup> Although most of the carbon atoms desorb, this surface should be classified as IIIA. From the presented results,  $(\sqrt{3} \times \sqrt{3})R30^\circ$  reconstruction also lies in IIIA category, while to-date  $(3 \times 3)$  reconstruction belongs to IIIB as a single member.

## V. CONCLUSION

The bonding strength between C<sub>60</sub> and both the  $(3 \times 3)$  and  $(\sqrt{3} \times \sqrt{3})R30^\circ$  reconstructions of  $6H$ -SiC(0001) was evaluated using IPES and LEED experiments. For  $(\sqrt{3} \times \sqrt{3})R30^\circ$  reconstruction, C<sub>60</sub> dissociates in a temperature range compatible with what is found for other Si-rich surfaces [Si(111)-(7 × 7) and Si(100)-(2 × 1)]. For the  $(3 \times 3)$  reconstruction, it is shown that C<sub>60</sub> desorbs at even higher temperature above 1100 K. Singularly, the nanostructured substrate is recovered and there is no evidence of C<sub>60</sub> dissociation. After desorption, the integrity of the Si-tetramers forming the  $(3 \times 3)$  reconstruction can be inferred on the basis of IPES.

This finding is unique among the previously studied Si surfaces, in the way that C<sub>60</sub> was always found to dissociate, forming a carbidic layer, when the bonding character is strong and predominantly covalent. We attribute this peculiar behavior to the low Si DB density of the  $(3 \times 3)$  reconstruction and to the highly corrugated character of this adcluster-based reconstruction.

This reversible covalent bonding illustrates again the richness of  $C_{60}$  chemistry at surfaces and has interesting implications for potential technological applications.  $C_{60}$  can, for instance, be used to passivate and protect the reactive  $(3 \times 3)$  reconstruction against contamination. If necessary, the removal of the protective layer can then be achieved under high vacuum using a simple high-temperature annealing up to 1100 K to recover the  $(3 \times 3)$ -reconstructed surface.

A patterning of the  $(3 \times 3)$  surface can also be envisioned using a high-temperature local-annealing process, e.g., laser induced.

#### ACKNOWLEDGMENTS

This work is supported by the ANR PNANO project MolSIC (ANR-08-P058-36).

\*jean-marc.themlin@im2np.fr

- <sup>1</sup>D. Nakamura, I. Gunjishima, S. Yamaguchi, T. Ito, A. Okamoto, H. Kondo, S. Onda, and K. Takatori, *Nature (London)* **430**, 1009 (2004).
- <sup>2</sup>W. A. de Heer *et al.*, *J. Phys. D: Appl. Phys.* **43**, 374007 (2010).
- <sup>3</sup>C. Cepek, P. Schiavuta, M. Sancrotti, and M. Pedio, *Phys. Rev. B* **60**, 2068 (1999).
- <sup>4</sup>M. Pedio *et al.*, *Phys. Scr.*, **T 115**, 695 (2005).
- <sup>5</sup>C.-P. Cheng, T.-W. Pi, C.-P. Ouyang, and J.-F. Wen, *J. Vac. Sci. Technol. A* **24**, 70 (2006).
- <sup>6</sup>P. J. Moriarty, *Surf. Sci. Rep.* **65**, 175 (2010).
- <sup>7</sup>S. J. Yao, C. G. Zhou, B. Han, T. Fan, J. P. Wu, L. Chen, and H. S. Cheng, *Phys. Rev. B* **79**, 155304 (2009).
- <sup>8</sup>A. J. Maxwell, P. A. Brühwiler, D. Arvanitis, J. Hasselström, M. K.-J. Johansson, and N. Mårtensson, *Phys. Rev. B* **57**, 7312 (1998).
- <sup>9</sup>S. Suto, K. Sakamoto, T. Wakita, C.-W. Hu, and A. Kasuya, *Phys. Rev. B* **56**, 7439 (1997).
- <sup>10</sup>P. Moriarty, M. D. Upward, A. W. Dunn, Y.-R. Ma, P. H. Beton, and D. Teehan, *Phys. Rev. B* **57**, 362 (1998).
- <sup>11</sup>L. Li, Y. Hasegawa, H. Shinohara, and T. Sakurai, *J. Vac. Sci. Technol. B* **15**, 1300 (1997).
- <sup>12</sup>F. Bechstedt, *Principles of Surface Physics* (Springer-Verlag, 2003).
- <sup>13</sup>U. Starke, J. Schardt, J. Bernhardt, M. Franke, K. Reuter, H. Wedler, K. Heinz, J. Furthmüller, P. Käckell, and F. Bechstedt, *Phys. Rev. Lett.* **80**, 758 (1998).
- <sup>14</sup>J. E. Northrup and J. Neugebauer, *Phys. Rev. B* **52**, R17001 (1995).
- <sup>15</sup>M. Rohlffing and J. Pollmann, *Phys. Rev. Lett.* **84**, 135 (2000).
- <sup>16</sup>F. Bechstedt and J. Furthmüller, *J. Phys. Condens. Matter* **16**, S1721 (2004).
- <sup>17</sup>M. B. Jost, N. Troullier, D. M. Poirier, J. L. Martins, J. H. Weaver, L. P. F. Chibante, and R. E. Smalley, *Phys. Rev. B* **44**, 1966 (1991).
- <sup>18</sup>V. Langlais, H. Belkhir, J.-M. Themlin, J.-M. Debever, L.-M. Yu, and P. A. Thiry, *Phys. Rev. B* **52**, 12095 (1995).
- <sup>19</sup>I. Forbeaux, J.-M. Themlin, and J.-M. Debever, *Phys. Rev. B* **58**, 16396 (1998).
- <sup>20</sup>G. Bertoni, C. Cepek, and M. Sancrotti, *Appl. Surf. Sci.* **212**, 52 (2003).
- <sup>21</sup>C. T. Tzeng, K. D. Tsuei, H. M. Cheng, and R. Y. Chu, *J. Phys. Condens. Matter* **19**, 176009 (2007).
- <sup>22</sup>A. Goldoni, R. Larciprete, C. Cepek, C. Masciovecchio, F. El Mellouhi, R. Hudej, M. Sancrotti, and G. Paolucci, *Surf. Rev. Lett.* **9**, 775 (2002).
- <sup>23</sup>J. R. Ahn, S. S. Lee, N. D. Kim, C. G. Hwang, J. H. Min, and J. W. Chung, *Surf. Sci.* **516**, L529 (2002).
- <sup>24</sup>C. Benesch, M. Fartmann, and H. Merz, *Phys. Rev. B* **64**, 205314 (2001).
- <sup>25</sup>J. Schardt, J. Bernhardt, U. Starke, and K. Heinz, *Phys. Rev. B* **62**, 10335 (2000).
- <sup>26</sup>J. Furthmüller, F. Bechstedt, H. Hüskén, B. Schröter, and W. Richter, *Phys. Rev. B* **58**, 13712 (1998).
- <sup>27</sup>L. S. O. Johansson, L. Duda, M. Laurenzis, M. Krieffewirth, and B. Reiherl, *Surf. Sci.* **445**, 109 (2000).
- <sup>28</sup>N. Troullier and J. L. Martins, *Phys. Rev. B* **46**, 1754 (1992).
- <sup>29</sup>J.-M. Themlin, S. Bouzidi, F. Coletti, J.-M. Debever, G. Genterblum, L.-M. Yu, J.-J. Pireaux, and P. A. Thiry, *Phys. Rev. B* **46**, 15602 (1992).
- <sup>30</sup>Y. R. Ma, P. Moriarty, M. D. Upward, and P. H. Beton, *Surf. Sci.* **397**, 421 (1998).
- <sup>31</sup>J. M. Themlin, I. Forbeaux, V. Langlais, H. Belkhir, and J. M. Debever, *Europhys. Lett.* **39**, 61 (1997).
- <sup>32</sup>J. E. Northrup and J. Neugebauer, *Phys. Rev. B* **57**, R4230 (1998).
- <sup>33</sup>V. Ramachandran and R. M. Feenstra, *Phys. Rev. Lett.* **82**, 1000 (1999).
- <sup>34</sup>A. Goldoni and G. Paolucci, *Surf. Sci.* **437**, 353 (1999).
- <sup>35</sup>K. Sakamoto, D. Kondo, H. Takeda, T. Sato, S. Suga, F. Matsui, K. Amemiya, T. Ohta, W. Uchida, and A. Kasuya, *Surf. Sci.* **493**, 604 (2001).
- <sup>36</sup>K. Sakamoto, D. Kondo, Y. Ushimi, M. Harada, A. Kimura, A. Kakizaki, and S. Suto, *Phys. Rev. B* **60**, 2579 (1999).
- <sup>37</sup>R. Hesper, L. H. Tjeng, and G. A. Sawatzky, *Europhys. Lett.* **40**, 177 (1997).